Behaviour of reinforced concrete affected by damage due to combined ASR and DEF: Assessment by NDT methods

Author: Goodluck Msigwa

Affiliation: Université de Toulouse; UPS, INSA; LMDC (Laboratoire Matériaux et Durabilité des Constructions); 135, avenue de Rangueil; F-31077 Toulouse Cedex 04, France. E-mail address: msigwa@insa-toulouse.fr

ABSTRACT: Alkali silica reaction (ASR) and delayed ettringite formation (DEF) are harmful swelling pathologies that have been observed in many reinforced concrete structures. It is particularly important to understand how expansion and damage due to the combination of the two pathologies affect the durability of reinforced concrete. Non-destructive testing (NDT) methods have been used in monitoring of swelling pathologies in concrete with an advantage of using the same specimens for several measurements. This research aims to understand the combined ASR and DEF damage effect in reinforced concrete by using NDT methods. Cylindrical plain and reinforced concrete specimens with diameter 160 mm, and height 320 mm were poured. The reinforcement ratios were 1 and 0.6% in longitudinal and transverse direction respectively. For monitoring, specimens were stored in tanks at 38^0 C while fully immersed in water. The specimens' expansions were measured by length comparators. The damage was assessed using linear and non-linear resonance vibration techniques and surface cracking observations also. Overall, dynamic modulus results from linear vibration showed that at same expansion, there is more damage in ASR alone than combined ASR and DEF pathologies. In addition, the linear vibration seems to be more sensitive than non-linear vibration at small expansions. For large expansion, the opposite trend was observed as the non-linear vibration seems to be more sensitive than the linear vibration. This shows the complementarity of the two NDT methods in monitoring ASR and DEF mechanisms.

Keywords: Alkali silica reaction (ASR), Delayed ettringite formation (DEF), Non-destructive testing methods (NDT), Reinforcement, Damage

1. INTRODUCTION

ASR and DEF are harmful swelling pathologies that occur in concrete structures threatening their structural integrity and durability. ASR is a reaction between different ionic species in concrete pore solution and reactive silica contained in aggregates (Rajabipour et al., 2015). It results in ASR products and causes expansion and cracking in concrete. DEF is a pathology that occurs when ettringite is formed after hardening of concrete due to high temperature curing $>65^0$ C causing expansion and cracking in concrete (Ingham, 2012). ASR and DEF mechanisms are influenced by factors such as concrete composition (cement, aggregates); environmental conditions (temperature, moisture); and stress conditions (restrains, creep). This paper focuses on the stress conditions effects particularly restraining by the presence of rebars.

Concrete stress conditions that affect ASR and DEF damage include shrinkage, creep and internal or external confinement. In a previous research on a C section large beam undergoing both ASR

and DEF simultaneously; the surface expansions in transverse direction were 3 times those in longitudinal direction due to the high amount of reinforcement in the longitudinal direction restraining the expansion (Karthik et al., 2016). In addition, the transverse reinforcement reached yield stress earlier than the longitudinal reinforcement resulting in more expansion and damage due to the combined effect of ASR and DEF. In another study on combined ASR and DEF on prestressed reinforced concrete beams, authors showed that the beams developed cracks but did not experience significant decrease in structural properties like bending stiffness, and ultimate load (Sanjeewa et al., 2024). The retaining of the structural properties was due to the restraining provided by prestress and rebars which restrained the ASR and DEF expansions. However, authors noted that in field structures, cracks generated can allow ingress triggering corrosion of rebars which can lead to loss of structural properties. Experimental studies dedicated to the mechanical evaluation of the combined effects of ASR and DEF damage on the structural behaviour of reinforced concrete structures are still necessary especially for laboratory small scale specimens.

NDT methods have several advantages such as they can be used on testing field structures without need of much coring. In addition, NDTs have advantages in the laboratory as they can be used multiple times to characterize one specimen thus reducing the overall scattering of results due to material variations (Balayssac and Garnier, 2018). Previous researches have shown successful use of linear and non-linear vibration methods in evaluating ASR and DEF pathologies in concrete with some limitations concerning the uniformity of the moisture content and the size of the specimens (Malone et al., 2021; Metalssi et al., 2015). This success inspired the usage of linear and non-linear vibration methods in this study.

Based on the highlighted literature, this study aims to investigate the effect of combined ASR and DEF damage on reinforced concrete by using NDT methods. For this purpose, plain and reinforced concrete specimens subjected to ASR and DEF expansion were poured and stored at 38^0 C while fully immersed in water. Thereafter, NDT methods of linear and non-linear vibration were used to monitor and characterize the damage resulting from the two pathologies. The novelty of this study lies in the understanding from the material and structural point of view on how damage due to ASR and DEF acts on reinforced concrete. In addition, this study aims to check the capability of NDT methods in evaluating damage in reinforced concrete structures affected by ASR and DEF pathologies.

2. METHODOLOGY

The methodology involved casting of plain and reinforced concrete specimens with a mix design representative of the concrete used in nuclear structures in France (Maalouf, 2024). Reactive and control mixes were cast into cylindrical specimens having 160 mm in diameter and 320 mm in height. Reactive concrete mix design had reactive siliceous limestone aggregates ranging from 4 to 20 mm in sieve size and cement containing 1% by weight of Na_2O_{eq} and 2.7% by weight of SO_3 mixed at water-to-cement ratio (w/c) of 0.56 (Table 1). In addition, NaOH was added to the mix at an amount of 1.9 kg per cubic meter of cast material to accelerate ASR. The control specimens were cast with the same mix design but with non-reactive limestone aggregates. The reinforcement configuration had 4 longitudinal rebars of diameter 8 mm achieving a reinforcement ratio of 1%

with stirrups also with diameter 8mm welded at 3 levels achieving a reinforcement ratio of 0.6% (Figure 1a).

After casting, the specimens subjected to ASR and DEF were placed in a climatic chamber for thermal treatment where temperature was gradually raised to 80^0 C and then gradually lowered to 20^0 C within 7 days to achieve the DEF pathology in parallel to ASR. The thermal treatment followed the LCPC lab methodology for concrete subjected to DEF (Pavoine and Divet, 2007). The ASR-only specimens were kept in autogenous conditions at 20^0 C for the 7 days period. Then after, all specimens were cured in autogenous conditions at 20^0 C for 28 days. Thereafter, all specimens were stored in tanks while fully immersed in water. In the first 21 days all specimens were immersed at 20^0 C to have stabilized saturation before gradually increasing the temperature to 38^0 C for monitoring.

Monitoring of the expansion was done by the length expansion and mass measurements using length comparator, outside micrometre and mass balance on 3 distinct specimens for each measurement (Figure 1b). The mechanical damage was assessed using linear and non-linear impulse excitation techniques inspired from previous researchers that used these methods for monitoring ASR (Lesnicki et al., 2013; Malone et al., 2021). Grindosonic equipment was used to obtain the linear frequencies (Figure 1c). The longitudinal and transverse (flexion) frequencies were obtained from the equipment and converted to dynamic elastic modulus following the ASTM C215-19 on saturated specimens (C09 Committee, 2020). Both longitudinal and transverse frequencies led to similar values of dynamic elastic modulus. OROS compact analyser equipment associated with NVGate software (Figure 1d) were used to obtain nonlinear parameter in transverse frequency mode. The output was frequencies and their corresponding accelerations which were then used for calculation of the non-linear parameter value with MATLAB software. The non-linear parameter α' which is associated to non-linear phenomena at mesoscopic scale was calculated according to equation 1, where; f_0 is the linear resonance frequency, f is the frequency at increased excitation amplitude (Leśnicki et al., 2011).

To validate the damage assessment results, surface cracking observations were done at the end of the monitoring. The monitoring of cracks opening on the exterior surface of the specimens was done using the Dino-Lite edge digital microscope with magnification range between 20 and 220 times (Figure 1e). During measurements, the microscope was calibrated using the calibration target at 40 times magnification. Then, magnified pictures of the cracks on the exterior surface of area 1 cm^2 of the specimens were taken using the dinocapture 3.0 software. Thereafter, the dimension line feature of the software was used to quantify the cracks opening by taking measurements of the width of cracks all along the whole crack length at about every 1 mm.

$$\frac{f_0 - f}{f_0} \sim \alpha' \tag{1}$$

TABLE 1. Concrete composition used for the reactive and control concretes

Concrete type	Constituents	Quantities (kg/m³)
Reactive	Cement CEM II/A-LL 42.5 R CE PM-CP2 NF	350
	Limestone sand (0-4 mm)	772
	Siliceous limestone gravel (4-14 mm)	316
	Siliceous limestone gravel (14-20 mm)	784
	Efficient water	195
	NaOH added	1.9
Control	Cement CEM II/A-LL 42.5 R CE PM-CP2 NF	350
	Limestone sand (0-4 mm)	772
	Limestone Gravel (4-14 mm)	316
	Limestone Gravel (14-20 mm)	784
	Efficient water	195
	NaOH added	1.9

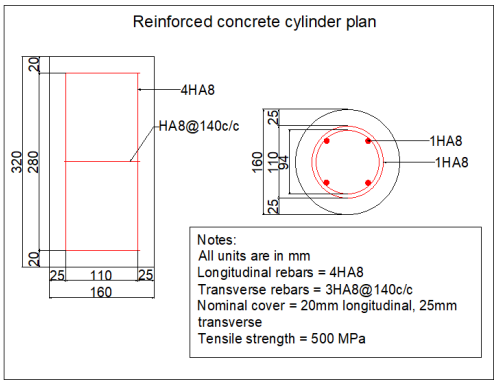

(a) longitudinal and transverse rebars details

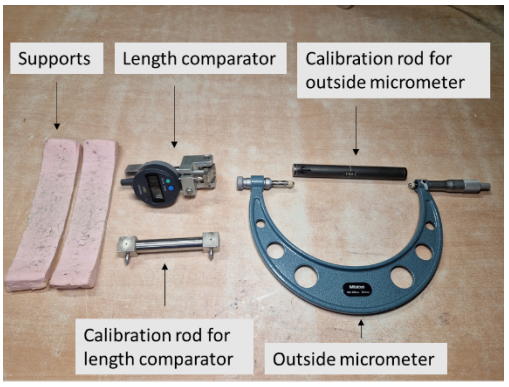

(b) Expansion measurement setup

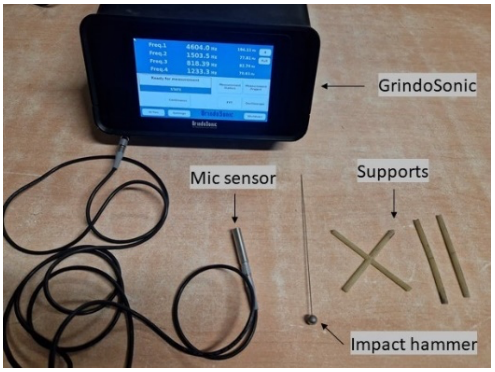

(c) Linear vibration technique setup

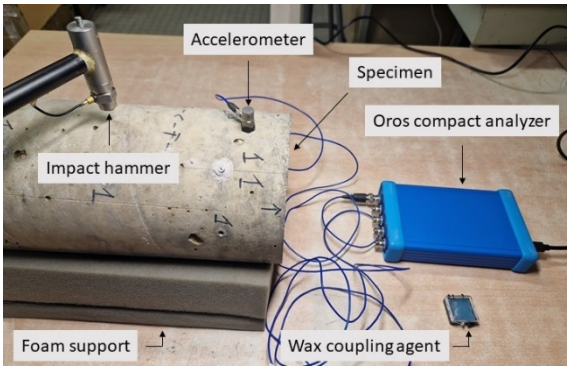

(d) Non-linear vibration technique setup

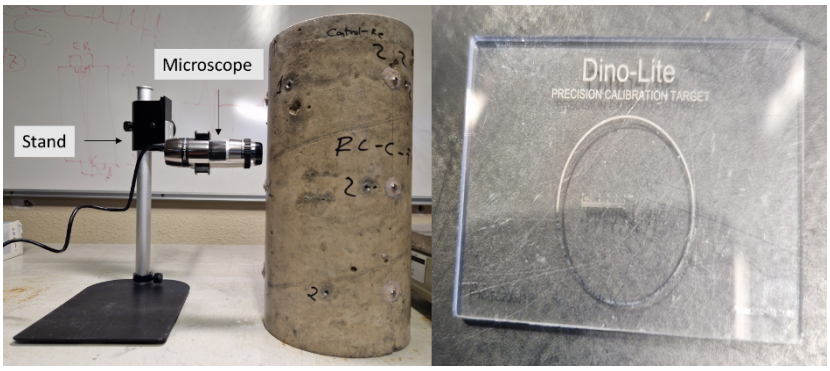

(e) Dino-lite microscope setup and the calibration target

FIGURE 1. The details and setup of measurements used in the methodology.

3. RESULTS

3.1 Length expansion

In the first 21 days after immersion in water at 20^{0}C, all specimens achieved an expansion in a range of 0.013 to 0.021% that was attributed to the water capillary imbibition. This attribute was verified by similar mass increase of 0.6% for both plain and reinforced ASR alone and control specimens. The plain and reinforced ASR and DEF specimens achieved a greater mass increase of 1% which was due to the early thermal treatment at 80^{0}C that altered the hydration products microstructure creating coarser pores that take more water (Lothenbach et al., 2007). Figure 2a shows the longitudinal expansion results after offsetting the expansion due to capillary imbibition. The deleterious threshold is the limit of 0.04% expansion above which ASR can cause structural deterioration and aggregates termed as reactive according to ASTM standards (C09 Committee, 2023). The effect of DEF is clearly seen as the plain specimens with a combination of ASR and DEF had a longitudinal expansion rate 3.75 times higher compared to ASR alone. In addition, the effect of longitudinal reinforcement is seen as the reinforced specimens subjected to ASR and DEF reached a maximum expansion that is only 27% of plain specimens. The reinforcement effect is also highlighted in the ASR alone as the reinforced specimens achieved maximum expansion that is only 50% that of plain specimens. In transverse expansion, the plain specimens undergoing ASR and DEF expansion exhibited an expansion rate 6 times higher compared to ASR alone (Figure 2b) highlighting the effect of DEF. Additionally, the reinforced specimens subjected to both ASR and DEF reached a maximum expansion that is only 60% of plain specimens which is the result of the transverse reinforcement. However, the transverse reinforcement effect is not present in ASR specimens as the reinforced and plain specimens have almost same expansion. When comparing longitudinal versus transverse expansions, the ASR alone plain specimens showed high anisotropy compared to ASR reinforced specimens. For ASR and DEF combination, the reinforced specimens had higher transverse than longitudinal expansion which is opposite trend for the plain specimens. Key observations to note here are amplification of expansion for combined ASR and DEF mechanisms, greater restraining effect on combined ASR and DEF specimens, shift of expansion to transverse direction for all reinforced specimens and high anisotropy of ASR alone specimens.

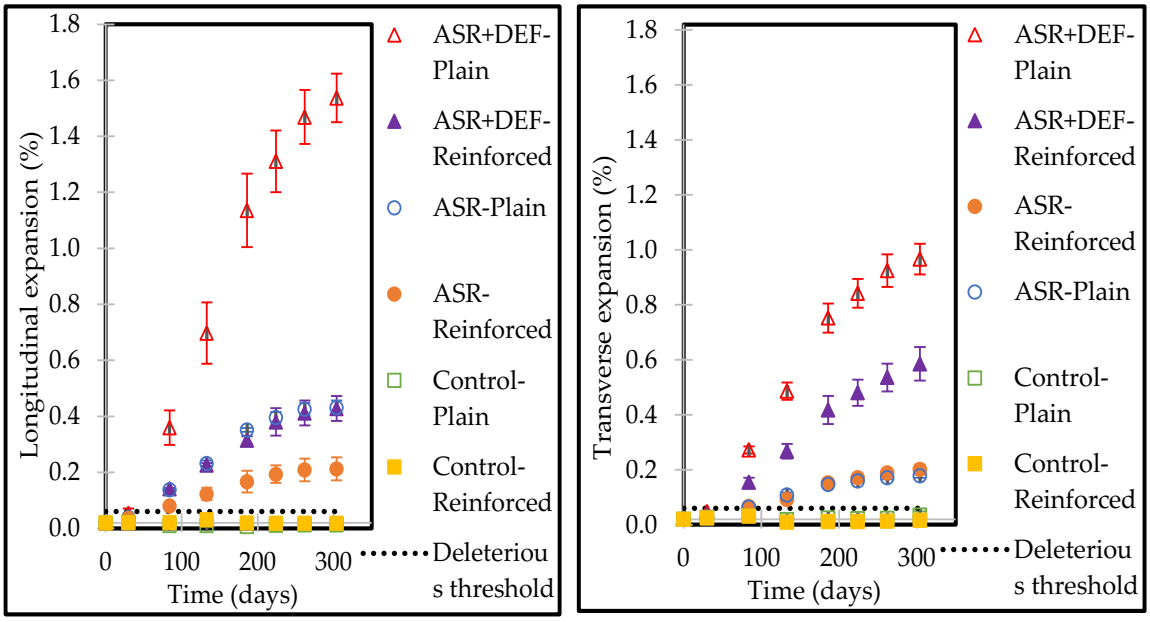

(a) Longitudinal (b) Transverse

FIGURE 2. (a) Longitudinal expansion (%) and (b) Transverse expansion (%) versus time (days) for all specimens

3.2 Dynamic elastic modulus

The dynamic elastic modulus increased for all specimens during the first 21 days of immersion in water at 20^{0}C which is attributed to the ongoing hydration of concrete and to the filling of the porosity by water. The results of longitudinal dynamic modulus after offsetting this increase are shown in Figure 3. The dynamic modulus for combined ASR/DEF plain and reinforced specimens was 10% lower compared to the ASR alone specimens since the beginning of the tests even before expansion. The control specimens had a slight increase in dynamic modulus over time due to ongoing hydration with reinforced ones achieving more higher dynamic modulus. The plain ASR and DEF specimens have the highest ultimate decrease in dynamic modulus which is as expected due to the highest expansion observed as shown in Figure 2. Another observation here is the stabilization and then beginning of slight gain in dynamic modulus at the end of expansion for all reactive specimens but more pronounced in ASR alone specimens.

The effect of restraint is seen in the ASR alone and combined ASR and DEF specimens, where, plain specimens have lower dynamic modulus compared to the reinforced specimens. However, the restraining effect is more pronounced in combined ASR and DEF mechanisms as it is twice that observed in the ASR alone mechanism. Key observations here are the low dynamic modulus in ASR and DEF specimens before pathologies expansion, lowest dynamic modulus for ASR and DEF specimens, gain in dynamic modulus at end of expansion especially for ASR alone pathology, and high restraining behaviour in combination of ASR and DEF pathologies compared to ASR alone pathology.

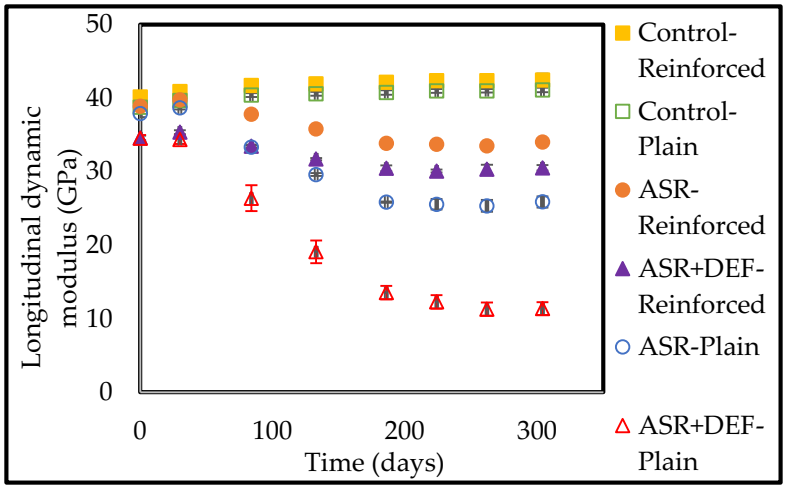

FIGURE 3. Longitudinal dynamic elastic modulus (GPa) versus time (days) for all specimens

3.3 Non-linear parameter range

The non-linear parameter ranges were stabilized in the beginning of the monitoring and started increasing for ASR alone and ASR and DEF specimens after about 100 days of monitoring (Figure 4). The non-linear parameter range increased the most for ASR and DEF plain specimens up to around 220 days and started stabilizing. For ASR alone plain specimens, the non-linear parameter range increased up to around 190 days and slightly decrease. The non-linear parameter range did not change significantly for reinforced reactive specimens and control specimens throughout the monitoring. In addition, the error bars increased with time of monitoring.

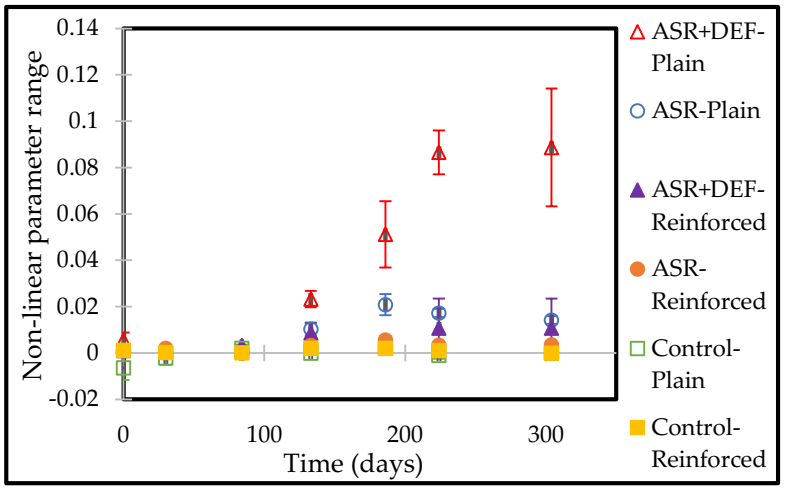

FIGURE 4. Non-linear parameter range versus time (days) for all specimens

3.4 Surface cracking observation

The surface cracking microscope images show that the plain specimens (Figure 5a and c) had horizontal cracking orientation that is perpendicular to the casting direction while the reinforced

specimens had vertical cracking orientation that is parallel to the longitudinal rebars (Figure 5b and d). The Figure 5 is a representation of crack opening for a few specimens. However, for all specimens, the reinforced specimens for ASR alone and ASR and DEF combination had cracks width of less than 400 µm which was less compared to the plain specimens showing the effect of restraining. In addition, the ASR and DEF combination in plain specimens had highest cracks width with most cracks having width above 800 µm compared to ASR alone plain specimens with most cracks with width of less than 400 µm and some with width between 400-800 µm. These results are consistent with results obtained for expansion in Figure 2.

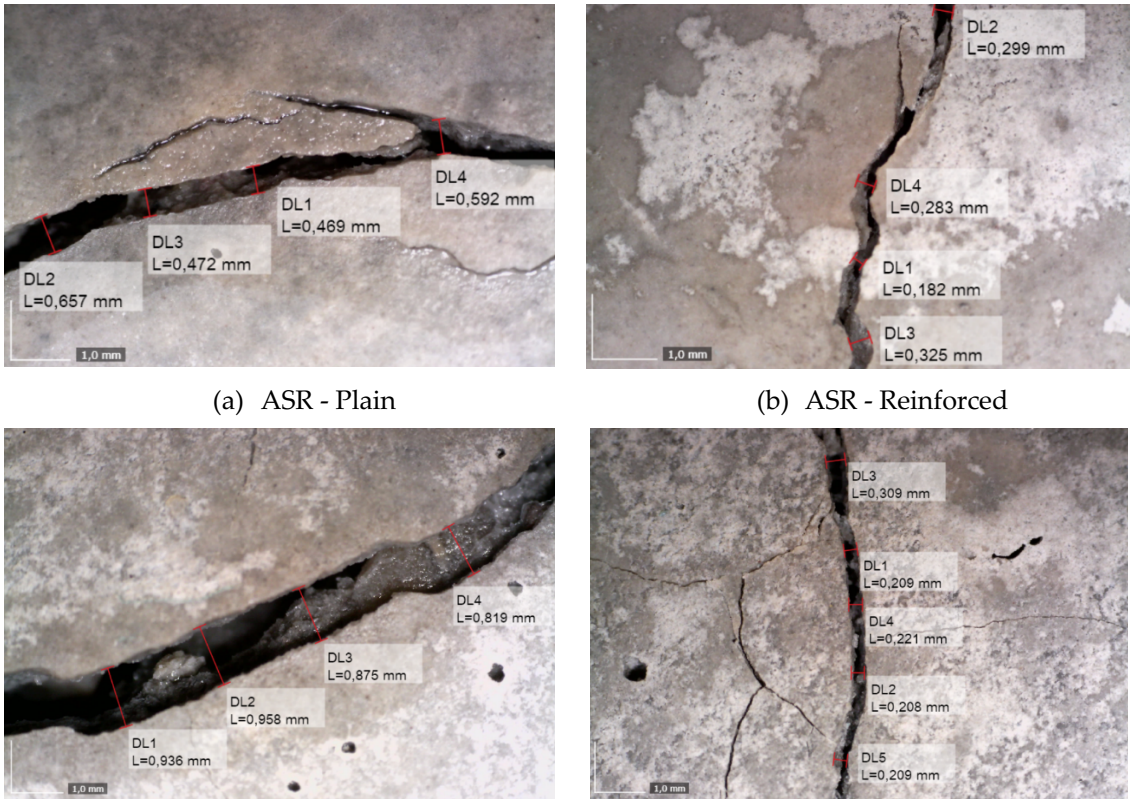

(a) ASR - Plain (b) ASR - Reinforced

(c) ASR+DEF - Plain (d) ASR+DEF - Reinforced

FIGURE 5. Surface cracking microscopic images for selected representative specimens of all configurations

4. DISCUSSION

4.1 ASR and DEF combined expansion

The combination of ASR and DEF reactions amplifies the expansion compared to ASR alone due to the combined pathologies acting together (Figure 2). Some authors have indicated that in combined ASR and DEF mechanisms, ASR occurs first where the ASR products lead to expansions and cause cracking in aggregates. Then the crystallized ettringite due to DEF fills and propagates the cracks causing more expansion and cracking both in cement paste and aggregate (Owsiak, 2010). Other authors have noted that DEF occurs first, where the crystallized ettringite forms the cracks and ASR

products flow into the cracks while also creating new cracks (Jensen and Sujjavanich, 2016). Regardless of which pathology occurs first, the presence of ASR or DEF amplifies the other causing more deleterious expansion than addition of ASR alone and DEF alone expansions (Sriprasong et al., 2020).

4.2 Restraint of expansion due to rebars

The low ASR and DEF expansions observed in reinforced specimens in Figure 2 is as expected. This is further shown in Figure 6a in longitudinal direction where points are below the equality line showing that reinforced specimens had low expansion compared to plain specimens for both ASR alone and combined ASR and DEF mechanisms. In addition, Figure 6b in transverse direction shows that the ASR alone points are close to the equality line showing that reinforced and plain specimens had similar expansions. The combined ASR and DEF specimens' points are below the equality line showing that reinforced specimens restrained expansions but in lower magnitude than in longitudinal direction. The effect of restraining is less in transverse direction due to shift of expansions to less restraint directions as the rebar ratio was only 0.6% in transverse direction compared to 1% in longitudinal direction. This further validates the crack patterns propagated in the direction parallel to the longitudinal rebars as seen in (Figure 5.b and d). This effect of shift of expansion has also been reported in previous researches of ASR in confined concrete (Multon and Toutlemonde, 2006; Wald et al., 2017).

Many previous researches have already shown that reinforcement restrains ASR or DEF expansions in structures (Jones and Clark, 1996; Morenon et al., 2017). One thing to note here however is how the rebars in combined ASR and DEF specimens restrain more expansion than rebars in ASR alone specimens. In longitudinal direction, rebars in combined ASR and DEF reactions led to a 73% reduction in expansion compared to ASR alone rebars that lead to only 50% expansion reduction. To understand this behaviour, stresses in concrete and steel rebars were calculated and plotted against time (Figure 7). It can be assumed that perfect bonding was obtained as the extremity of the longitudinal rebars has been welded on the transversal rebars (**Erreur ! Source du renvoi introuvable.**a). From the Figure 7, the combined ASR and DEF reaction leads to high tensile stress in steel that in turn leads to high compressive stress in concrete therefore restraining more expansions compared to ASR alone. For example, at around 140 days, the compressive stress in ASR and DEF concrete is already at 4 MPa compared to only 2 MPa in ASR alone concrete. Further analysis of the Figure 7 shows that ASR alone reaction never led to rebars yielding. The combined ASR and DEF reaction led to rebar yielding around 160 days. This led to stabilization of rebars effect as there is minimal increase in stress during rebars plasticity phase. This stabilization of rebars effect should have led to modification of expansion as there is minimal restraint available. However, at this stage of the reaction there are already cracks formed hence the new products might be moving to these cracks instead of forming new ones that would have led to expansion increase. Another reason for the high restraining behaviour in ASR and DEF reaction compared to ASR alone can be that in ASR, cracks begin in aggregates (Sanchez et al., 2015) which are more rigid. While, for DEF cracks begin in cement paste (Taylor et al., 2001) which are less rigid thus becoming less effective in creating expansion in presence of rebars. In summary, several mechanisms can be occurring simultaneously to explain the difference of restraint of expansion.

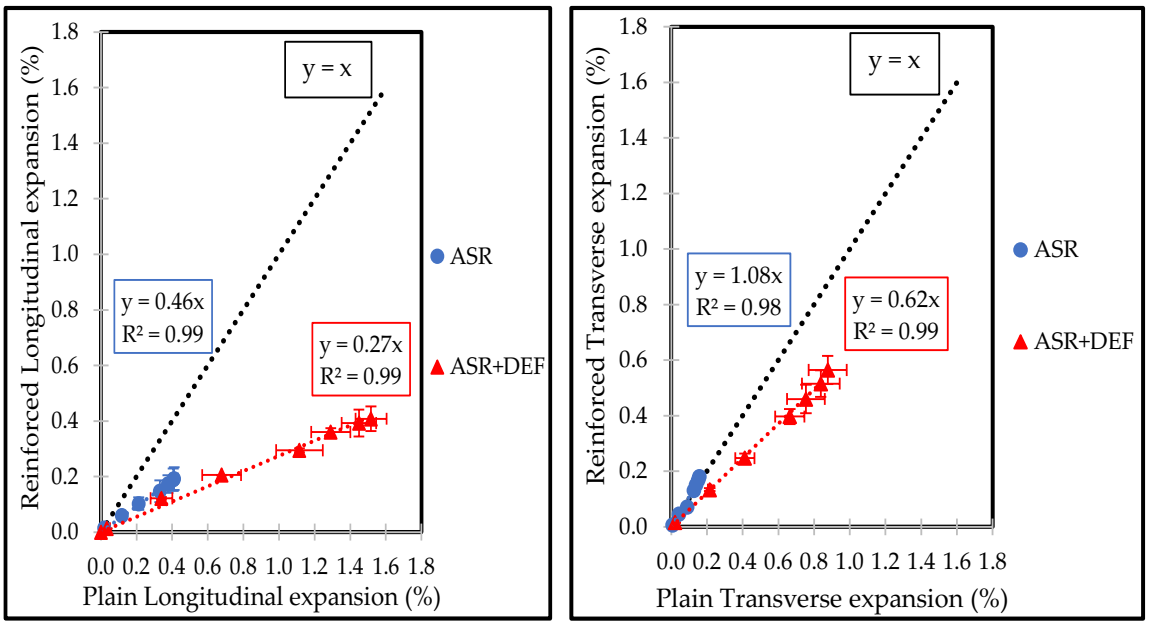

(a) Longitudinal (b) Transverse

FIGURE 6. Reinforced versus plain expansion (%) in (a) longitudinal and (b) transverse directions.

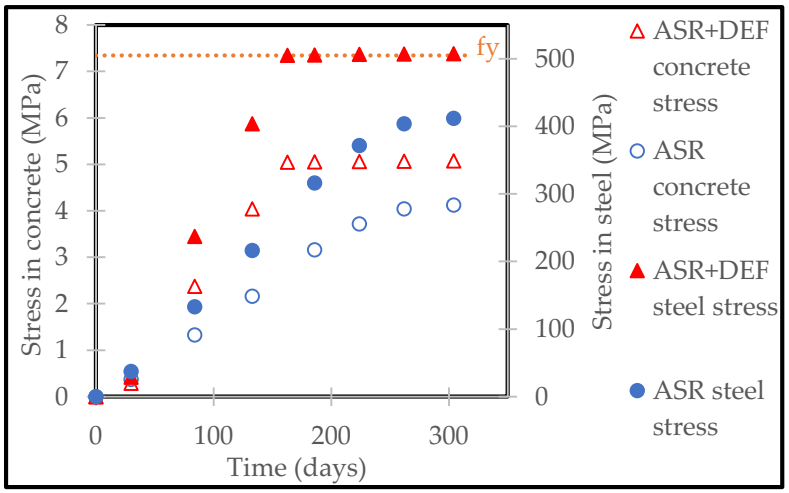

FIGURE 7. Stresses in concrete and steel (MPa) in longitudinal direction versus time (days)

4.3 Anisotropy and isotropy

To further analyse the anisotropy and isotropy behaviour, the longitudinal versus transverse expansion for all specimens are plotted in Figure 8. All plain specimens are above the equality line showing anisotropy which is more pronounced in ASR alone specimens. The reinforced specimens are at the equality line or slightly below showing no anisotropy. This is consistent with expansion behaviour in Figure 2 and cracking observations in Figure 5. Previous studies have shown that ASR

is anisotropic while DEF is isotropic (Bouzabata et al., 2012). In this study, looking at the plain specimens, ASR specimens showed anisotropy as expected. The combination of ASR and DEF also showed anisotropy although to a lesser degree than ASR alone specimens. The anisotropy observed in ASR and DEF combination can be due to that ASR occurred first consequently influencing the crack pattern as seen in Figure 5.c where the widest cracks are perpendicular to the casting direction. Another reason for the anisotropy observed can be due the specimen aspect ratio of 2:1 hence influencing the cracking perpendicular to the slender dimension due to effect of diffusive mechanisms such as alkali leaching or water diffusion.

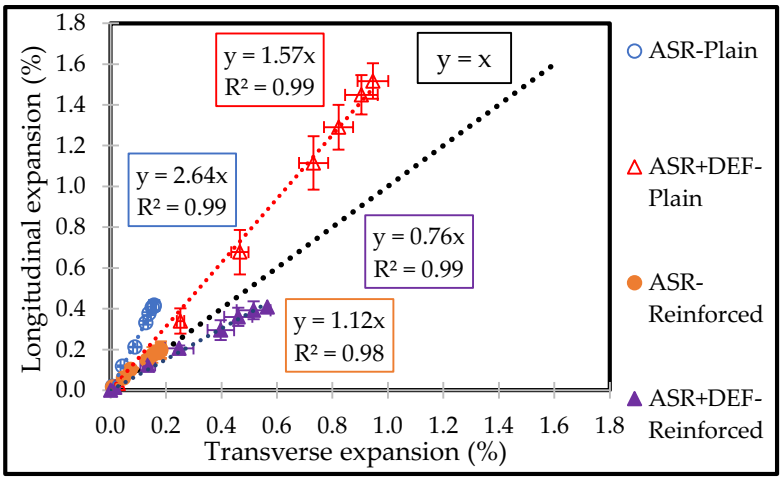

FIGURE 8. Longitudinal versus transverse expansion (%) for all specimens

4.4 Damage behaviour

The damage observed in ASR and DEF combination in Figure 3 can be grouped in two phenomena. First is the damage observed at the beginning of monitoring which is due to early age conditions and then the damage observed later in the monitoring which is due to ASR and DEF expansions. At early age, the ASR and DEF specimens were exposed to temperatures up to 80^{0}C. The specimens were kept in a climatic chamber with controlled conditions to ensure homogenous thermal treatment and saturation. The controlled conditions reduced shrinkage and thermal damage risk but heating the specimens at up to 80^{0}C led to some modification of hydration products. Higher temperatures in concrete at early age lead to denser hydration products that are more heterogeneously distributed creating coarser pores that lead to decrease in concrete mechanical properties (Lothenbach et al., 2007). Later in the monitoring, the highest damage observed in ASR and DEF specimens is due to ASR and DEF expansions and this is further validated by the wider cracks in ASR and DEF specimens compared to ASR alone specimens as observed in Figure 5.

To further analyse the damage behaviour, the normalized dynamic modulus values were plotted against the expansion (Figure 9). From the figure, it can be seen again that at the end of expansion, there is a stabilization and a slight increase in the dynamic modulus which is more pronounced in the ASR alone specimens. This slight increase in dynamic modulus can be due to that as ASR continues, ASR products formed can fill the existing cracks hence having an effect similar to hydration of increase in concrete mechanical properties (Joo and Takahashi, 2024).

Further analysis of the Figure 9 shows that for expansions below 0.4%, at same expansion level, the ASR alone specimens had more damage compared to combination of ASR and DEF specimens. This behaviour was same for both plain and reinforced specimens. This behaviour shows that the pathologies expansions cannot be directly linked to the loss in mechanical properties which was also observed in another previous research (Miura et al., 2022). At small expansions, two hypotheses can be proposed for the combined ASR and DEF mechanisms. First is that as the ASR occurs and cracking begins in aggregates, the ettringite formed after dissolution of monosulphates fills these cracks as a consequence less damage observed at time of testing. A previous study has shown that for concrete exposed in humid environment, re-crystallization of unstable phases in cement paste can occur leading to precipitation of secondary ettringite in cracks which does not cause further expansion or cracking (Johansen et al., 1993). This might be the case in this study as the concrete was fully immersed in water at 100% saturation degree. Second hypothesis is that DEF reaction begins by forming closed cracks in cement paste and around aggregates (Taylor et al., 2001) before expanding and causing further cracking unlike ASR that begins by forming open cracks in aggregates (Sanchez et al., 2015). Hence, the open cracks cause detection of more loss in dynamic modulus than the closed cracks. Both hypotheses are linked to the microstructure of the concrete thus requiring further microstructural analysis for validation. These analyses will be done in the next paper.

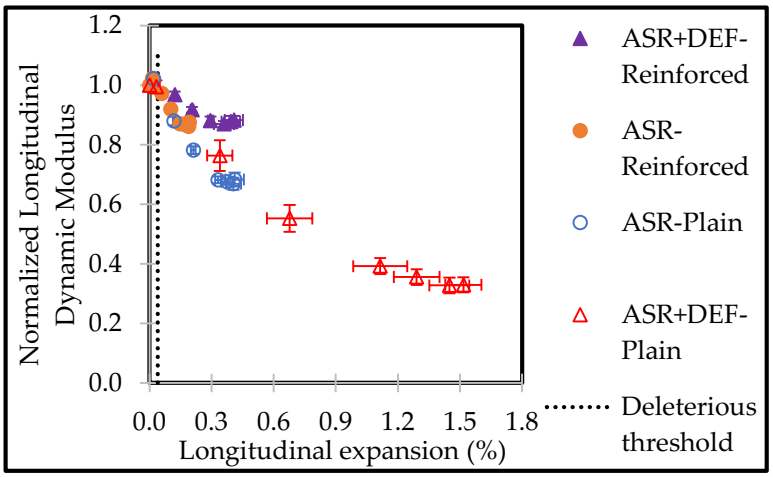

FIGURE 9. Normalized dynamic modulus versus longitudinal expansion (%) for reactive specimens

4.5 Comparison between linear and non-linear vibration techniques

An increase in non-linear parameter range means more damage at mesoscopic scale is occurring as there is a bigger shift of frequencies with the increase of applied vibration amplitude. In Figure 4, the non-linear parameter did not change in the beginning but later after 100 days showing that it was insensitive in the beginning of monitoring at small expansions less than 0.2% but more sensitive later in monitoring at large expansions. This behaviour is in contrast with linear vibration method which showed it was more sensitive in the beginning of monitoring at small expansion than later

at large expansions. The combination usage of linear and non-linear vibration can be a complementarity in monitoring ASR and DEF pathologies full damage history.

5. CONCLUSION

This research involved a study on the behaviour of reinforced concrete undergoing damage due to combined ASR and DEF mechanisms by utilizing NDT methods. In addition, the study aimed to check the capability of NDT methods in characterizing ASR and DEF mechanisms. The concrete was casted into cylindrical specimens and restrained at 1 and 0.6% of rebars ratio in longitudinal and transverse directions. Then specimens were monitored while conditioned at temperature of 38^0C and fully immersed in water. The measurements done were length expansion, linear and non-linear free-resonance vibration and surface cracking analysis. The length expansion results showed the amplification of expansion due to combined ASR and DEF reactions. Additionally, they highlighted high restraining effect on combined ASR and DEF mechanisms and a shift of expansion to transverse direction which had less restraining effect compared to the longitudinal direction. The dynamic modulus results exhibited gain in dynamic modulus at end of expansion and at same expansion, lower damage in combined ASR and DEF pathologies compared to ASR alone. In addition, the rebars restrained damage as the reinforced specimens result in higher dynamic modulus compared to the plain specimens. Interesting discussions on the results have been highlighted and some hypotheses proposed that will be useful in the understanding of combined ASR and DEF mechanisms damage on reinforced concrete. Further microstructural analyses will be done for the next paper to validate the hypotheses proposed. Lastly, the linear vibration showed more sensitivity than non-linear vibration at small expansions. For large expansion, the opposite trend was observed as the non-linear vibration showed more sensitivity than the linear vibration due to the development of damage at mesoscopic scale. This shows the complementarity of the two NDT methods in monitoring ASR and DEF mechanisms from beginning at small expansions to end at large expansions. Further analysis and development of the linear and non-linear vibration methods used in this study is required so that they can be used in monitoring ASR and DEF pathologies in field structures.

REFERENCES

Balayssac, J.-P., Garnier, V., 2018. Évaluation non destructive des ouvrages en génie civil, Illustrated édition. ed. ISTE Editions, Londres.

Bouzabata, H., Multon, S., Sellier, A., Houari, H., 2012. Swellings due to alkali-silica reaction and delayed ettringite formation: Characterisation of expansion isotropy and effect of moisture conditions. Cem. Concr. Compos. 34, 349–356. https://doi.org/10.1016/j.cemconcomp.2011.10.006

C09 Committee, 2023. Test Method for Determination of Length Change of Concrete Due to Alkali-Silica Reaction. https://doi.org/10.1520/C1293-20A

C09 Committee, 2020. Test Method for Fundamental Transverse, Longitudinal, and Torsional Resonant Frequencies of Concrete Specimens. ASTM International. https://doi.org/10.1520/C0215-19

Ingham, J., 2012. Briefing: Delayed ettringite formation in concrete structures. Proc. Inst. Civ. Eng. - Forensic Eng. 165, 59–62. https://doi.org/10.1680/feng.12.00001

Jensen, V., Sujjavanich, S., 2016. ASR AND DEF IN CONCRETE FOUNDATIONS IN THAILAND.

Johansen, V., Thaulow, N., Skalny, J., 1993. Simultaneous presence of alkali — silica gel and ettringite in concrete. Adv. Cem. Res. 5, 23–29. https://doi.org/10.1680/adcr.1993.5.17.23

Jones, A.E.K., Clark, L.A., 1996. The effects of restraint on ASR expansion of reinforced concrete. Mag. Concr. Res. 48, 1–13. https://doi.org/10.1680/macr.1996.48.174.1

Joo, H.E., Takahashi, Y., 2024. Crack-filling effect of gel on time-dependent mechanical behavior of concrete damaged by alkali–silica reaction. Mater. Struct. 57, 45. https://doi.org/10.1617/s11527-024-02308-y

Karthik, M.M., Mander, J.B., Hurlebaus, S., 2016. Deterioration data of a large-scale reinforced concrete specimen with severe ASR/DEF deterioration. Constr. Build. Mater. 124, 20–30. https://doi.org/10.1016/j.conbuildmat.2016.07.072

Lesnicki, K.J., Kim, J.-Y., Kurtis, K.E., Jacobs, L.J., 2013. Assessment of alkali-silica reaction damage through quantification of concrete nonlinearity. Mater. Struct. 46, 497–509. https://doi.org/10.1617/s11527-012-9942-y

Leśnicki, K.J., Kim, J.-Y., Kurtis, K.E., Jacobs, L.J., 2011. Characterization of ASR damage in concrete using nonlinear impact resonance acoustic spectroscopy technique. NDT E Int. 44, 721–727. https://doi.org/10.1016/j.ndteint.2011.07.010

Lothenbach, B., Winnefeld, F., Alder, C., Wieland, E., Lunk, P., 2007. Effect of temperature on the pore solution, microstructure and hydration products of Portland cement pastes. Cem. Concr. Res. 37, 483–491. https://doi.org/10.1016/j.cemconres.2006.11.016

Maalouf, J., 2024. Perméabilité à l'air du béton armé endommagé par des Réactions de Gonflement Interne (RGI) (phdthesis). Université de Toulouse.

Malone, C., Zhu, J., Hu, J., Snyder, A., Giannini, E., 2021. Evaluation of alkali–silica reaction damage in concrete using linear and nonlinear resonance techniques. Constr. Build. Mater. 303, 124538. https://doi.org/10.1016/j.conbuildmat.2021.124538

Metalssi, O.O., Godart, B., Toutlemonde, F., 2015. Effectiveness of Nondestructive Methods for the Evaluation of Structures Affected by Internal Swelling Reactions: A Review of Electric, Seismic and Acoustic Methods Based on Laboratory and Site Experiences. Exp. Tech. 39, 65–76. https://doi.org/10.1111/ext.12010

Miura, T., Sato, K., Fujishima, M., Nakamura, H., Kawabata, Y., 2022. Mechanism for reduction in compressive properties of cementitious materials in relation to internal crack patterns due to ASR and DEF expansion. Cem. Concr. Compos. 128, 104441. https://doi.org/10.1016/j.cemconcomp.2022.104441

Morenon, P., Multon, S., Sellier, A., Grimal, E., Hamon, F., Bourdarot, E., 2017. Impact of stresses and restraints on ASR expansion. Constr. Build. Mater. 140, 58–74. https://doi.org/10.1016/j.conbuildmat.2017.02.067

Multon, S., Toutlemonde, F., 2006. Effect of applied stresses on alkali-silica reaction-induced expansions. Cem. Concr. Res. 36, 912–920. https://doi.org/10.1016/j.cemconres.2005.11.012

Owsiak, Z., 2010. THE EFFECT OF DELAYED ETTRINGITE FORMATION AND ALKALI-SILICA REACTION ON CONCRETE MICROSTRUCTURE. Ceram. – Silikáty.

Pavoine, A., Divet, L., 2007. Méthode d'essai n°66 Réactivité d'un béton vis-à-vis d'une reaction sulfatique interne. Laboratoire Central des Ponts et Chaussées.

Rajabipour, F., Giannini, E.R., Dunant, C.F., Ideker, J.H., Thomas, M.D.A., 2015. Alkali-silica reaction: Current understanding of the reaction mechanisms and the knowledge gaps. Cem. Concr. Res. 76, 130–146. https://doi.org/10.1016/j.cemconres.2015.05.024

Sanchez, L.F.M., Fournier, B., Jolin, M., Sorelli, L., Duchesne, J., 2015. Reliable quantification of AAR damage through assessment of the Damage Rating Index (DRI). Cem. Concr. Res. 67, 74–92. https://doi.org/10.1016/j.cemconres.2014.08.002

Sanjeewa, H.V.A.N., Matsumoto, A., Asamoto, S., Martin, R.-P., Toutlemonde, F., 2024. Experimental study on flexural behaviour of DEF–ASR-affected prestressed concrete beams. Eng. Struct. 319, 118835. https://doi.org/10.1016/j.engstruct.2024.118835

Sriprasong, T., Asamoto, S., Raj, J.N., 2020. Study on the Combined Alkali Silica Reaction and Delayed Ettringite Formation. Int. J. Geomate 19, 84–91. https://doi.org/10.21660/2020.75.38051

Taylor, H.F.W., Famy, C., Scrivener, K.L., 2001. Delayed ettringite formation$. Cem. Concr. Res.

Wald, D.M., Allford, M.T., Bayrak, O., Hrynyk, T.D., 2017. Development and multiaxial distribution of expansions in reinforced concrete elements affected by alkali-silica reaction. Struct. Concr. 18, 914–928. https://doi.org/10.1002/suco.201600220